反应与分离

DOI: 10.12034/j.issn.1009-606X.219342

Performance and modelling of bromide dynamic adsorption onto D301 anion exchange resin

Chunyi YUAN[1,2], Yuzhu SUN[1,2,3*], Ying YANG[1,2], Xingfu SONG[1,2], Jianguo YU[1,2*]

1. National Engineering Research Center for Integrated Utilization of Salt Lake Resource, East China University of Science and Technology, Shanghai 200237, China
2. Engineering Research Center of Resources Process Engineering, Ministry of Education, Shanghai 200237, China
3. Shanghai Institute of Pollution Control and Ecological Security, Shanghai 200092, China

Abstract: The adsorption of bromide ions from the mother liquor produced during the process of mining potassium from rock-salt mines onto D301 anion exchange resin in a Perspex column was investigated. Relevant breakthrough curves were obtained, which would provide valuable information for the process design at a real scale. Experiments were carried out to study the effects of the initial adsorbate concentration, bed length, and flow rate. The bed capacities were found to increase with increasing initial adsorbate concentration and decreasing flow rate. When the initial Br^- concentration increased from 1000 mg/L to 4000 mg/L, the adsorption capacity increased from 1.8 mg/mL to 6.4 mg/mL. The breakthrough time and the exhaust time increased with increasing bed length and decreasing flow rate, whereas they remained almost the same when changing the initial adsorbate concentration. Five adsorption models, including Bed Depth Service Time (BDST), Thomas, Yoon-Nelson, Wolborska and Modified dose response (MDR) were applied to predict the breakthrough curves and to determine the characteristic parameters of fixed-bed column. The MDR model was found to be the best fit to the experimental data. This study indicates that the D301 anion exchange resin can be used to extract bromide ions from mother liquors effectively in the competition with high concentrations of chloride ions.

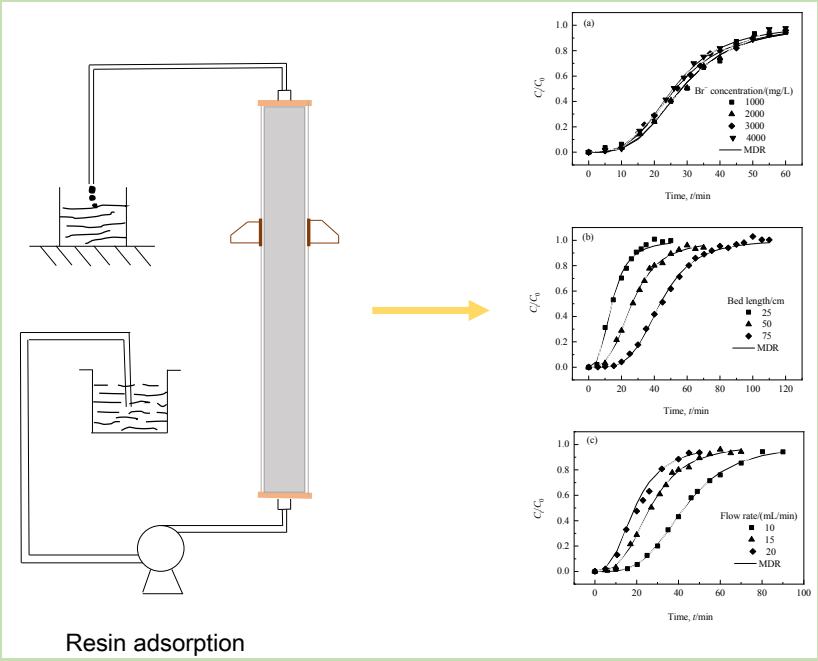

Key words: anion exchange resin; breakthrough curve; bromine; modelling; Modified dose response model

Received: 2019−11−12, **Revised:** 2020−01−19, **Published online:** 2020−02−12
Foundation item: National Key R&D Program of China (No. 2016YFC0401203); Program of Shanghai Academic/Technology Research Leader (No. 18XD1424600)
Biography: Chunyi YUAN(1995−), female, Qidong County, Jiangsu Province, master student, major in chemical engineering; corresponding authors, Yuzhu SUN, E-mail: yzsun@ecust.edu.cn, Jianguo YU, E-mail: jgyu@ecust.edu.cn.

引用格式: Yuan C Y, Sun Y Z, Yang Y, et al. Performance and modelling of bromide dynamic adsorption onto D301 anion exchange resin. Chin. J. Process Eng., 2020, 20(6): 655−666, DOI: 10.12034/j.issn.1009-606X.219342.

D301 树脂动态吸附溴离子过程探究及模型拟合

袁纯怡[1,2]， 孙玉柱[1,2,3*]， 杨 颖[1,2]， 宋兴福[1,2]， 于建国[1,2*]

1. 国家盐湖资源综合利用工程技术研究中心，华东理工大学，上海 200237
2. 资源过程工程教育部工程研究中心，上海 200237
3. 上海污染控制与生态安全研究院，上海 200092

摘 要：研究了用 D301 树脂吸附岩盐矿提钾母液中溴离子的可能性，考察了吸附柱动态吸附过程中原料液溴离子初始浓度、床层高度及进料流速等因素的影响。结果表明，增加原料液溴离子初始浓度或降低进料流速能提高树脂单位饱和吸附量。当原料液溴离子初始浓度从 1 000 mg/L 升至 4 000 mg/L 时，树脂单位饱和吸附量从 1.8 mg/L 增至 6.4 mg/mL。增加床层高度或降低进料流速会延长动态吸附突破时间及饱和时间，而原料液溴离子初始浓度对其没有影响。应用了 Bed Depth Service Time(BDST), Thomas, Yoon-Nelson, Wolborska 及 Modified dose response(MDR)等五种吸附模型对动态吸附过程进行拟合，其中 MDR 模型的拟合效果最佳。D301 树脂可用于从含有高浓度氯离子的提钾母液中提取溴离子。

关键词：阴离子交换树脂；突破曲线；溴；模型拟合；Modified dose response 模型

中图分类号：O647.3 **文献标识码**：A **文章编号**：1009-606X(2020)06–0655–12

1 INTRODUCTION

Bromine is an important raw material in the chemical industry, and can be used in the production of materials such as fire retardants, medicines, photosensitive materials, military products and so on[1,2]. The main sources of bromine are seawater, subsurface brine, saline lake brine and so on. There are many limitations during the production of bromine due to the properties of the sources, production cost and so on. Meanwhile, bromine is always in short supply because of its scarcity and uneven global distribution, resulting in high prices[3]. Therefore, research into improved methods for the extraction and utilization of bromine is required.

The rock-salt mines in Southeast Asia are mainly mined for potassium and magnesium. However, the concentration of bromine in the mother liquor produced during the flotation process for extracting potassium is rather high compared to that in the sea (65 mg/L) or in the brines in China (49~1 680 mg/L)[4], which is around 3 000 mg/L[5,6]. As a result, it is meaningful to extract the bromine from the recycled mother liquor to make better use of the mine resources.

Current processes applied for the extraction of bromide ions include air blow-out, steam distillation, membrane separation and so on[7–10]. Bromide ions need to be oxidized to bromine in these processes, and acidification is an essential step in order to inhibit the hydrolysis of bromide during oxidation. However, the potassium liquor in rock salt deposit brine has to be solidified and backfilled after the production by adding alkaline materials. Acidification not only increases the cost of the process, but also pollutes the environment. Hence, it is important to develop a new process which can extract the bromide ions directly from the mother liquor without acidification and oxidation.

To the best of our knowledge, no previous work on the extraction of bromide ions with high concentration directly has been reported in the literature. In this study, adsorption by anion exchange resin (AER) was taken as an alternative technology to extract the bromide ions directly based on previous studies. Harada et al. [11] found that bromide ions can be tightly bound by the ion-exchange sites. Wang[12] and Phetrak et al.[13] used AERs to adsorb bromide ions from sea water and drinking water source respectively, in which the concentrations of bromide were 65 and 0.125 mg/L.

In our previous work, D301 resin was selected as the most suitable resin in adsorption of bromide ions from the mother liquor of KCl in batch mode among seven

commercial anion exchange resins, which had quick adsorption, the highest adsorption capacity, the lowest cost and ease of desorption. From the industrial point of view, fixed-bed column adsorption experiments should be carried out to obtain valuable parameters for scaling up. However, such practices were time consuming and costly, so that accurate modeling and simulation were frequently used as an alternative for predicting the dynamic behavior of fixed-bed systems to optimize column design and operation parameters[14–16]. The main objective of this present work was devoted to the kinetic study of the adsorption of bromide ions from the mother liquor of KCl, which was a saturated $MgCl_2$ solution, onto D301 resin in a fixed-bed column experiment as well as by computer simulations. The effects of the initial adsorbate concentration, bed length, and flow rate were studied by five adsorption models. The Bed Depth Service Time (BDST)[17–19], Thomas[20–22], Yoon-Nelson[23–25], Worborska[26,27], and Modified dose response models[28] were applied to the experimental data to predict the breakthrough curves and determine related parameters. This study of chromatographic separation of bromide ions by adsorption in fixed-bed columns packed with D301 resin can develop a new method for bromine separation and provide theoretical knowledge on designing devices for industrial production.

2 MATERIALS AND METHODS

2.1 Materials

D301 anion exchange resin was used in the study. The resin is styrene based with ternary ammonium functional group, and its main properties are given in Table 1.

All the chemicals used in the preparation of the adsorbate solutions were of analytical reagent grade. The basis of the adsorbate solutions was $MgCl_2$, having a mass fraction around 27%. There were also small amounts of NaCl and KCl in the industrial solutions depending on the actual production, typically 2wt%~3wt%. The concentration of Br^- ranges from 1 000 to 4 000 mg/L in this study, and it was adjusted by adding different amounts of NaBr.

2.2 Batch Adsorption

Table 1 Properties of D301 anion exchange resin

Property	Value
Appearance	Beige, bead
Moisture/%	48~58
Capacity/(mmol/g)	4.8
Apparent density/(g/mL)	0.65~0.72
BET surface area/(m^2/g)	36.48

Batch experiments were carried out for equilibrium studies by contacting certain quantity of resin with adsorbate solutions with different concentrations of NaBr. The concentrations of Br^- were set as 500, 1 000, 1 500, 2 000, 2 500, 3 000, 3 500, 4 000, 4 500 and 5 000 mg/L respectively, while the concentrations of $MgCl_2$, NaCl and KCl remained the same.

After reaching the adsorption equilibrium, the suspension was filtered through cellulose nitrate membranes (0.45 μm), and the concentration of bromide was determined. The amount of bromide adsorbed onto a mass unit of wet resin (q_e, mg/g) was calculated by the equation:

$$q_e = \frac{(C_0 - C_e)V}{m} \quad (1)$$

where C_0 and C_e are the concentrations of bromide in the aqueous solution (mg/L) at the initial stage and at equilibrium time, respectively, V is the volume of the solution (L), and m is the weight of the wet resin (g). Experiments were performed in triplicate.

2.3 Column Studies

The performance of the D301 anion exchange resin in adsorbing Br^- was studied using a Perspex column, of which the internal diameter was 2.5 cm and the length was 50 cm. The adsorbate solution was fed from the bottom of the column, which was packed with D301 anion exchange resin, using a peristaltic pump. A beaker was placed at the outlet of the column to avoid the loss of the effluent and samples were collected at certain time intervals for analysis. The initial Br^- concentration varied from 1 000 mg/L to 4 000 mg/L, the inlet flow rate varied from 10 mL/min to 20 mL/min and the bed height varied from 25 cm to 75 cm. All experiments were conducted at room temperature. The concentration of Br^- in the samples were measured by ICP (ICP-OES, spectra ARCOS, Germany).

3 THEORY

3.1 Adsorption Isotherm

It is important to establish the adsorption isotherm, which can be used to predict the adsorption parameters reliably, compare the adsorption performance at different conditions and optimize the design of an adsorption system. Two classic adsorption isotherm models, Langmuir[29] and Freundlich[30], were used to fit the experimental data in the study.

The Langmuir isotherm is shown in the following equation.

$$q_e = \frac{q_m K_L c_e}{1 + K_L c_e} \tag{2}$$

where q_m is the monolayer adsorbent capacity under equilibrium conditions (mmol/g), which indicates the maximum concentration retained by the adsorbent surface when it is completely covered by an adsorbate monolayer, K_L is the Langmuir constant (L/mmol).

The Freundlich isotherm model can be expressed by the form:

$$q_e = K_F C_e^{\frac{1}{n}} \tag{3}$$

where K_F gives an estimate of the adsorption capacity of the adsorbent [$\text{mmol}^{(n-1)/n}\cdot\text{L}^{(1/n)}$/g], $1/n$ is a temperature dependent parameter, which shows if the adsorption is favorable or not.

3.2 Breakthrough Curves

The fixed-bed column mode consists in continuously feeding an influent containing a target substance into a column packed with a particular adsorbent[31]. The concentration of the target substance at the outlet of effluent stream would increase gradually during the adsorption process, until it equals to the concentration of the inlet stream. Therefore, the breakthrough curves are obtained by plotting the normalized concentration, C_t/C_0 versus time or volume throughout, where C_t and C_0 are the concentration of the outlet stream at the certain time and the inlet stream respectively. The general formula for calculating the amount of the target substance adsorbed onto the adsorbent (q_t) at the certain time was calculated by numerical integration of the area above the breakthrough curve using the following equation[32]:

$$q_t = Q \cdot C_0 \int_0^t (1 - \frac{C_t}{C_0}) \mathrm{d}t \tag{4}$$

3.3 Fixed-bed Column Models

The prediction of the breakthrough curves is essential to attain a successful fixed-bed adsorption design. In this work, five established models, BDST, Thomas, Yoon-Nelson, Wolborska and MDR, were used to fit the experimental data in order to determine relevant parameters to predict the breakthrough curves and subsequently determine the influence for optimization of the fixed-bed adsorption process.

3.3.1 Bed depth service time (BDST) model

The BDST model is based on the assumption that the rate controlling step in the adsorption process is the surface reaction while the intraparticle mass transfer resistance and the external film resistance can be ignored[19]. It gives a relationship between the bed height and service time in terms of adsorption parameters such as flow rate, process concentration and so on. The specific equation is as follows:

$$t = \frac{N_0 H}{C_0 U} - \frac{1}{K_0 C_0} \ln\left(\frac{C_0}{C_t} - 1\right) \tag{5}$$

where H is the bed height (cm), t is the service time (min), U is the linear velocity (cm/min), N_0 is the adsorption capacity (mg/L), K_0 is the rate constant of the model [L/(mg·min)], C_0 is the inlet solution concentration (mg/L), and C_t is the outlet solution concentration at time t (mg/L). This equation can be converted as follow:

$$\frac{C_t}{C_0} = \frac{1}{\exp\left(\frac{K_0 N_0 H}{U} - K_0 C_0 t\right) + 1} \tag{6}$$

So that the rate constant of the model (K_0) and the adsorption capacity (N_0) can be determined through plotting C_t/C_0 versus t at certain bed height, flow rate, and inlet solution concentration.

3.3.2 Thomas model

The Thomas model is one of the most widely used model in column performance analysis. The maximum bed adsorption capacity of a column is one of the parameters needed in the successful design and the Thomas model is used to fulfill the purpose[33]. Thomas model is especially suitable for adsorption processes that

follow the Langmuir isotherm for equilibrium and second-order reversible reaction kinetics[20]. It assumes a constant separation factor but is applicable to both favorable and unfavorable adsorption conditions. The main constraint of this model is that external and internal diffusion limitations are absent in its assumption. Thomas model can be expressed as follows:

$$\frac{C_t}{C_0}=\frac{1}{\exp\left(\frac{K_T q_0 m}{Q}-K_T C_0 t\right)+1} \tag{7}$$

where K_T is the Thomas rate constant [L/(min·mg)], q_0 is the equilibrium adsorbate uptake (μg/mL), m is the mass of adsorbent in the column (g), and Q is the volumetric flow rate (mL/min).

The Thomas rate constant (K_T) and the equilibrium adsorbate uptake (q_0) can be determined after fitting the experimental data to the model.

3.3.3 Yoon-Nelson model

The Yoon-Nelson model is a relatively simple model and does not require detailed data about the adsorbate, adsorbent, and the adsorption bed. It is based on the assumption that the rate of decrease in the possibility of adsorption for each adsorbate molecule is proportional to the possibility of adsorbate adsorption and the possibility of adsorbate breakthrough on the adsorbent[23]. The Yoon-Nelson equation is expressed as follow:

$$\frac{C_t}{C_0}=\frac{1}{\exp(K_{YN}\tau-K_{YN}t)+1} \tag{8}$$

where K_{YN} is the equation rate constant (min^{-1}), τ is the time required for 50% adsorbate breakthrough (min). These two parameters can be determined by using nonlinear regression.

3.3.4 Wolborska model

The Wolborska model is often used to describe the concentration distribution in an adsorption bed for the low-concentration range of the breakthrough curve[27]. The applicable relative concentration range is usually up to 0.5. The equation is expressed as follow:

$$\frac{C_t}{C_0}=\exp\left(\frac{\beta C_0 t}{N_0}-\frac{\beta Z}{U}\right) \tag{9}$$

where β is the kinetic coefficient of external mass transfer (min^{-1}) and Z is the bed height (cm).

The kinetic coefficient of external mass transfer (β) and the adsorption capacity (N_0) can be determined through plotting (C_t/C_0) versus t in certain adsorption process.

3.3.5 Modified dose response (MDR) model

The Modified dose response model is another simplified model that can be used to evaluate dynamic behaviors of an adsorption bed[34]. The key point of Modified dose response model is that it matches the breakthrough curve better than other models like the Thomas model, especially when the relative concentration is low or high. The equation can be written as follow:

$$\frac{C_t}{C_0}=1-\frac{1}{1+\left(\frac{C_0 Q t}{q_0 m}\right)^a} \tag{10}$$

where a is the parameter of the Modified dose response model and the other symbols have their usual meanings.

The constant of the Modified dose response model (a) and the equilibrium adsorbate uptake (q_0) can be determined after fitting the experimental data to the model.

4 RESULTS AND DISCUSSION

4.1 Equilibrium Adsorption

Equilibrium data concerning the adsorption of bromide onto D301 anion exchange resin is shown in Figure 1. It shows that the isotherm is linear in the range of concentration studied, which indicates that the amount of bromide absorbed is much smaller than the adsorption capacity of the resin and the adsorption sites are not fully

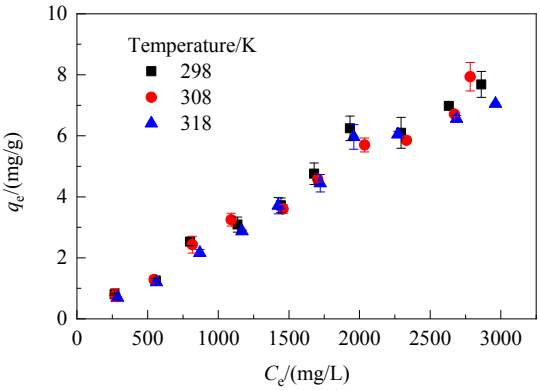

Fig.1　Experimental results of isotherms at different temperatures

Table 2 Isothermal line model fitting parameters at different temperatures

T/K	Langmuir			Freundlich		
	K_L/(L/mmol)	q_m/(mmol/g)	R^2	K_F/[mmol$^{(n-1)/n}$·L$^{(1/n)}$/g]	n	R^2
298	0.004	0.802	0.726	0.003	1.009	0.980
308	0.005	0.567	0.683	0.003	1.019	0.988
318	0.005	0.553	0.601	0.002	0.951	0.990

utilized. Therefore, the increase of the concentration brings the increase of the amount adsorbed. Besides, it can be seen that the temperature has little effect on the adsorption.

The equilibrium data were fitted to Langmuir and Freundlich models and the adsorption isotherms parameters are shown in Table 2. It can be seen from the correlation coefficients that Freundlich model gave a better fit to the experimental adsorption data than Langmuir equation, which indicated that the surface of the adsorbent was not uniform due to the micropores and pipes in the resin. The values of K_F also showed that the temperature had little effect on the adsorption.

4.2 Effect of Initial Adsorbate Concentration

Experiments were carried out at different initial adsorbate concentrations, and the flow rate and bed length were constant at 15 mL/min and 50 cm. The influence of various initial Br^- concentration on the adsorption process is shown in Figure 2. The parameters obtained from the breakthrough curves at different initial concentrations are presented in Table 3. In the present study, the breakthrough time and the exhaust time correspond to C_t/C_0=0.1 and 0.9, respectively. It was illustrated in Figure 2 that the breakthrough curves changed little when the initial Br^- concentration increased from 1000 mg/L to 4000 mg/L. Therefore, adsorption processes at different initial concentrations had similar breakthrough time, exhaust time and volume of the treated solutions (V_{eff}). Meanwhile, the equilibrium adsorbate uptake (q_0) increased with increasing initial concentration proportionally. These results were in line with the linear isotherm obtained in former study. It indicated that in this range of initial concentrations, the mass transfer resistance did not change much when changing the concentration[34]. On the other hand, more bromide ions were absorbed per gram of adsorbent at a higher initial concentration due to the fact that higher concentration of inlet solution bringed higher Br^- loading rate[23].

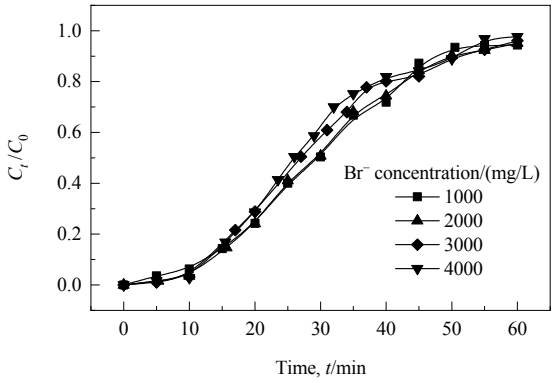

Fig.2 Effect of initial Br^- concentration on breakthrough curve (flow rate=15 mL/min and bed length=50 cm)

Table 3 Parameters obtained from breakthrough curves of adsorption processes at different initial Br^- concentrations

C_0/(mg/L)	H/cm	Q/(mL/min)	t_b/min	t_{total}/min	V_{eff}/mL	q_0/(mg/mL)
1000	50	15	12.5	46.5	697.5	1.8
2000	50	15	13.5	50	750	3.9
3000	50	15	13	51	765	4.6
4000	50	15	13	51	765	6.4

4.3 Effect of Bed Length

Figure 3 shows the breakthrough curves obtained at various bed lengths, with a constant flow rate of 15 mL/min and initial Br^- concentration of 3000 mg/L, respectively. It can be seen obviously that with the increase of the bed length, both the breakthrough time and the exhaust time increased, and the specific values are listed in Table 4. This was an expected result because when the bed length was increased, the adsorbent load would also increase, and hence, the total adsorption

capacity of the bed would increase. As a result, more time would be needed for breakthrough and exhaustion. The equilibrium adsorbate uptake remained almost the same when increasing the bed length in the adsorption process. It was regarded that as the bed height increased, more resin was packed, and the length for the adsorption was larger, resulting in higher column capacity utilization[32].

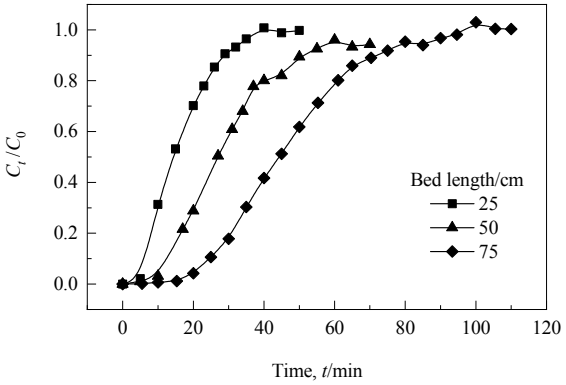

Fig.3　Effect of bed length on breakthrough curve (flow rate=15 mL/min and initial Br^- concentration=3 000 mg/L)

4.4 Effect of Flow Rate

Flow rate is another important factor when analyzing the performance of adsorption processes. Therefore, experiments were carried out to identify the effect of flow rate by varying it between 10 and 20 mL/min. During these experiments, the initial Br^- concentration and bed height were maintained at 3 000 mg/L and 50 cm, respectively. The breakthrough curves for bromide adsorption at various flow rates are shown in Figure 4. Related parameters obtained from the breakthrough curves are shown in Table 5.

Table 4　Parameters obtained from breakthrough curves of adsorption processes at different bed lengths

C_0/(mg/L)	H/cm	Q/(mL/min)	t_b/min	t_{total}/min	V_{eff}/mL	q_0/(mg/mL)
3000	25	15	6.7	28.6	429	4.7
3000	50	15	13	51	765	4.6
3000	75	15	24.5	72	1080	4.7

The breakthrough curves show that an increase in the flow rate at a constant bed length decreases the breakthrough time. This can be explained by the fact that the increase of the flow rate results in an increase in the mass transfer rate, thus accelerating the adsorption process. Therefore, breakthrough occurs earlier at higher flow rates. It can be observed from Table 5 that the equilibrium adsorbate uptake decreases with the increase in the flow rate. As the flow rate increases, the contact time between adsorption zone and solution decreases. Hence, the ions do not have sufficient time to diffuse into the pores of adsorbents through intra-particle diffusion. On the other hand, at lower flow rate, the residence time of the adsorbate in the adsorption bed would increase and bromide ions have more time to penetrate and diffuse deeply into the pores[24]. As a result, more bromide ions will be absorbed per gram of adsorbent, resulting in a delayed exhaust time.

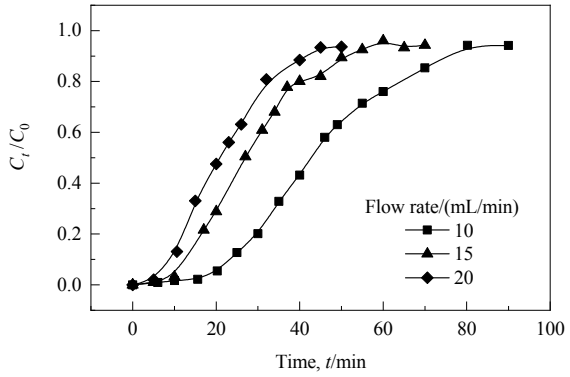

Fig.4　Effect of flow rate on breakthrough curve (bed length=50 cm and initial Br^- concentration=3 000 mg/L)

Table 5　Parameters obtained from breakthrough curves of adsorption processes at different flow rates

C_0/(mg/L)	H/cm	Q/(mL/min)	t_b/min	t_{total}/min	V_{eff}/mL	q_0/(mg/mL)
3000	50	10	23	74.5	745	4.9
3000	50	15	13	51	765	4.6
3000	50	20	9.5	41.5	830	3.5

4.5 Column Modelling

In this study, experimental data were fitted to five adsorption models, BDST, Thomas, Yoon-Nelson, Wolborska, and Modified dose response, to identify the

best model to describe the adsorption kinetics and determine relevant parameters, which were crucial for the process design.

4.5.1 Analysis using BDST, Thomas, and Yoon-Nelson models

The BDST, Thomas, and Yoon-Nelson models can all be written as follow:

$$\frac{C_t}{C_0}=\frac{1}{\exp(b-dt)+1} \tag{11}$$

where $b=K_0N_0H/U$ (BDST model), k_Tq_0m/Q (Thomas model), or $K_{YN}\tau$ (Yoon-Nelson model), while $d=K_0C_0$ (BDST model), k_TC_0 (Thomas model), or K_{YN} (Yoon-Nelson model). These three models share the same theoretical breakthrough curves, and thus the same correlation coefficient (R^2) and the sum of the squares of the differences (SSE). A comparison of the experimental and theoretical breakthrough curves for the adsorption process using the three models are shown in Figure 5. Table 6 lists the values obtained along with the correlation coefficient and the sum of the squares of the differences.

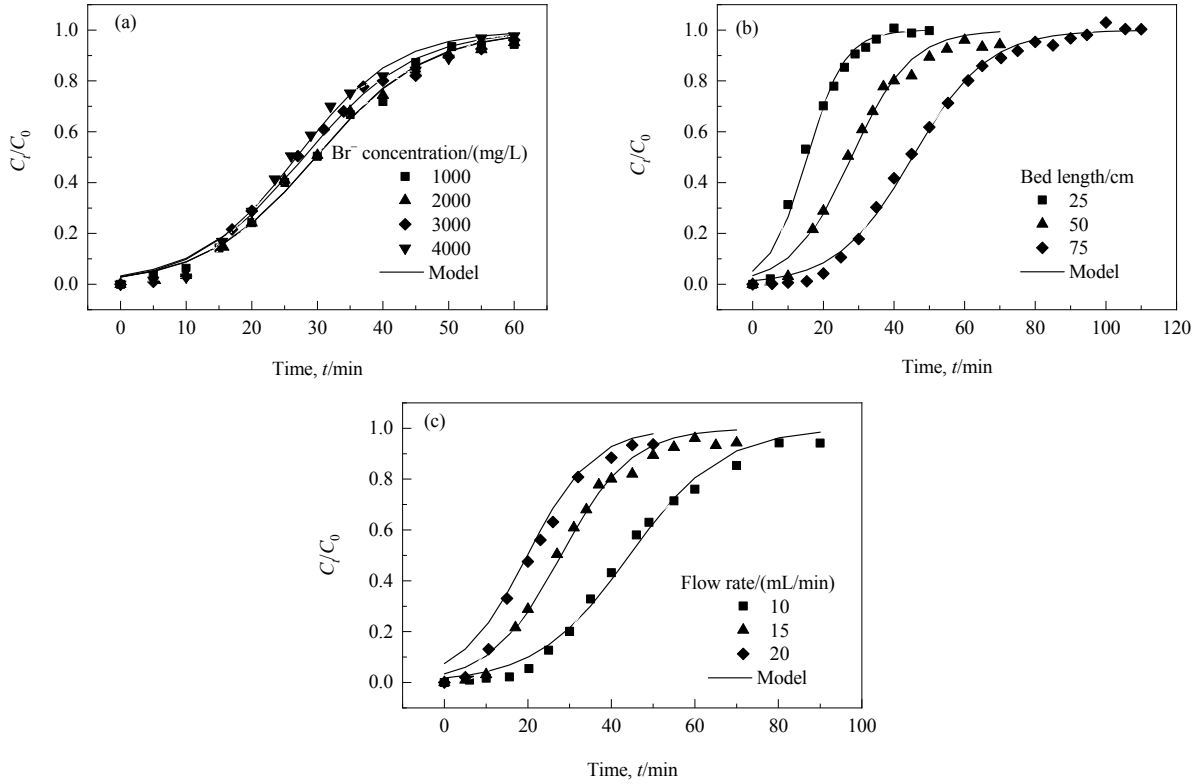

Fig.5 Comparisons of experimental and theoretical breakthrough curves for the adsorption process using the BDST, Thomas and Yoon-Nelson models

Table 6 Parameters of the BDST, Thomas and Yoon-Nelson models for bromide adsorption

C_0/(mg/L)	H/cm	Q/(mL/min)	K_0 (BDST)/[×10⁻⁵ L/(mg·min)]	N_0 (BDST)/(mg/L)	K_T (Thomas)/[×10⁻⁵ L/(mg·min)]	q_0 (Thomas)/(mg/mL)	K_{YN} (Yoon-Nelson)/min	τ (Yoon-Nelson)/min	R^2	SSE
1000	50	15	9.43	2229	9.43	3.18	0.12	29.76	1.00	0.0075
2000	50	15	5.17	4094	5.17	5.85	0.12	29.73	0.99	0.011
3000	50	15	4.06	4998	4.06	7.14	0.12	27.96	0.99	0.019
4000	50	15	3.25	6521	3.25	9.32	0.13	26.80	0.99	0.021
3000	25	15	6.37	5464	6.37	7.81	0.19	17.30	0.99	0.021
3000	75	15	3.20	5128	3.20	7.33	0.09	45.25	1.00	0.013
3000	50	10	3.07	5231	3.07	7.47	0.09	44.32	0.99	0.018
3000	50	20	4.30	4691	4.30	6.70	0.13	19.87	0.99	0.017

As shown in Figure 5, the models agree well with the experimental data in the relative concentration range of 0.2 to 0.8. For lower or higher relative concentration, the correlation between the experimental and predicted values is not ideal. This is probably due to the fact that these models are more suitable for adsorption processes that follow the Langmuir isotherm for equilibrium[20] while the experimental adsorption data in this study is fit to Freundlich isotherm rather than Langmuir isotherm.

The rate constant (K_0) and the adsorption capacity (N_0) in the BDST model were obtained after fitting. With increasing initial concentration, the rate constant decreased but the adsorption capacity increased. This is due to the fact that the adsorbate molecules have more driving force in the competition for the adsorption site with higher adsorbate concentrations, which results in more adsorbate adsorbed.

The rate constant (K_T) and the equilibrium adsorbate uptake (q_0) in the Thomas model are also given in Table 6. The value of K_T is the same as K_0 in the BDST model and the trend of q_0 matches with that of N_0 in BDST model. The rate constant decrease with increasing C_0 and decreasing Q, whereas the equilibrium adsorbate uptake would increase under the same condition. Thus, with a higher initial concentration of the inlet solution and a lower flow rate, the adsorption of Br^- onto the D301 anion exchange resin will increase.

The equation rate constant (K_{YN}) and the time required for 50% adsorbate breakthrough (τ) in the Yoon-Nelson model were also obtained. These values showed that the rate constant increased with decreasing bed length and increasing flow rate, whereas the time required for 50% adsorbate breakthrough decreased with increasing flow rate and decreasing bed length. Furthermore, the rate constant and the time required for 50% adsorbate breakthrough remained almost the same with the change in initial concentration, which is consistent with the experimental observations. The values of τ obtained agreed well with the experimental data. This is also supported by the high value of correlation coefficient R^2.

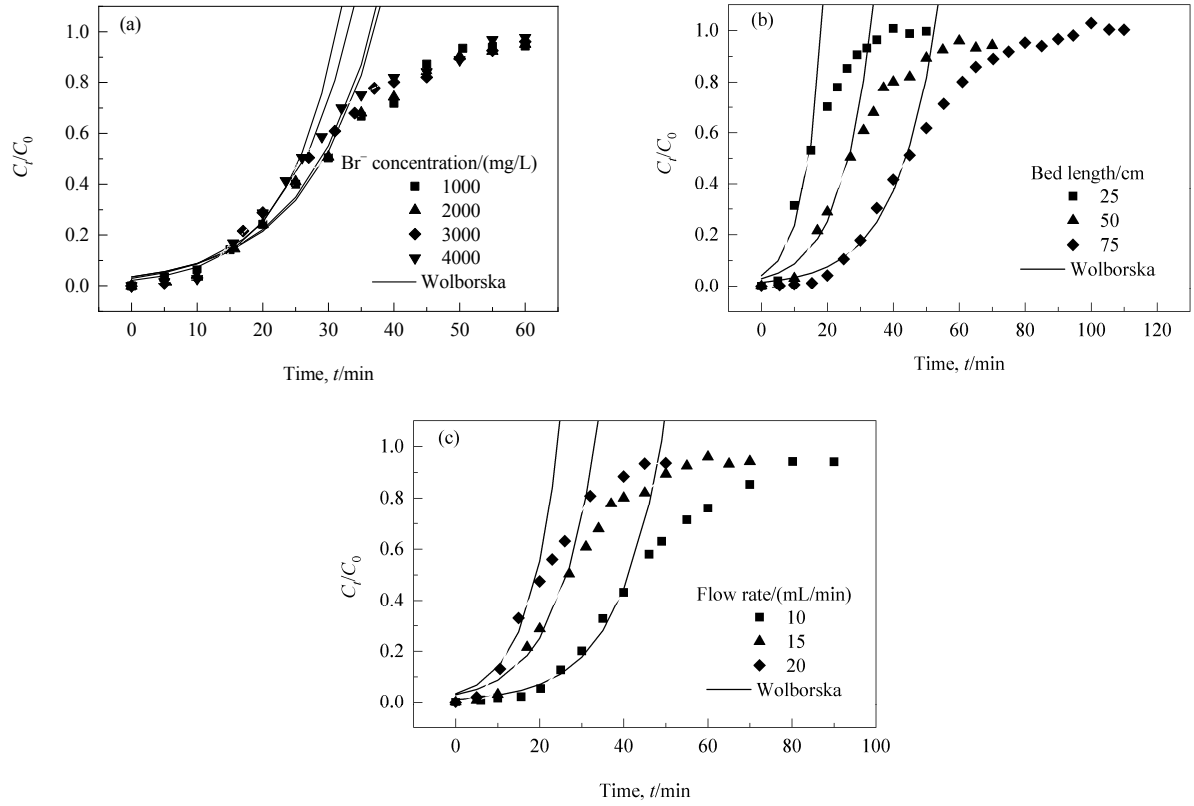

Fig.6　Comparisons of experimental and theoretical breakthrough curves for the adsorption process using the Wolborska model

4.5.2 Analysis using Wolborska model

The Wolborska model was used in this study for the relative concentration ranging from 0 to 0.5 since it is more suitable for the low-concentration range of the breakthrough curve[27]. The theoretical breakthrough curves obtained are shown in Figure 6 for comparison with the experimental curves. Relevant parameters are listed in Table 7. It can be seen that the kinetic coefficient of external mass transfer (β) increased with the decrease of bed height and the increase of flow rate. This is because the turbulence increases when increasing the flow rate or decreasing the bed height, which would reduce the film boundary layer surrounding the resin particles[22]. In addition, the value of β changed little with changing initial concentration, whereas the adsorption capacity (N_0) increased continuously with increasing initial concentration. This is consistent with the earlier discussion of this range of initial concentration, that is, the mass transfer resistance will not change significantly when changing the concentration and more bromide ions will be absorbed with increasing initial concentration as a result of the higher Br^- loading rate. The fitting between the curves was not ideal, which can be observed from the values of correlation coefficient R^2 listed in Table 7.

Table 7 Parameters of the Wolborska model for bromide adsorption

C_0/(mg/L)	H/cm	Q/(mL/min)	β/min	N_0/(mg/L)	R^2	SSE
1000	50	15	0.20	2779	0.97	0.0074
2000	50	15	0.20	5030	0.96	0.012
3000	50	15	0.21	5903	0.96	0.0087
4000	50	15	0.23	7606	0.98	0.006
3000	25	15	0.34	5816	0.93	0.014
3000	75	15	0.16	5957	0.97	0.011
3000	50	10	0.18	5754	0.98	0.0041
3000	50	20	0.27	5721	0.95	0.01

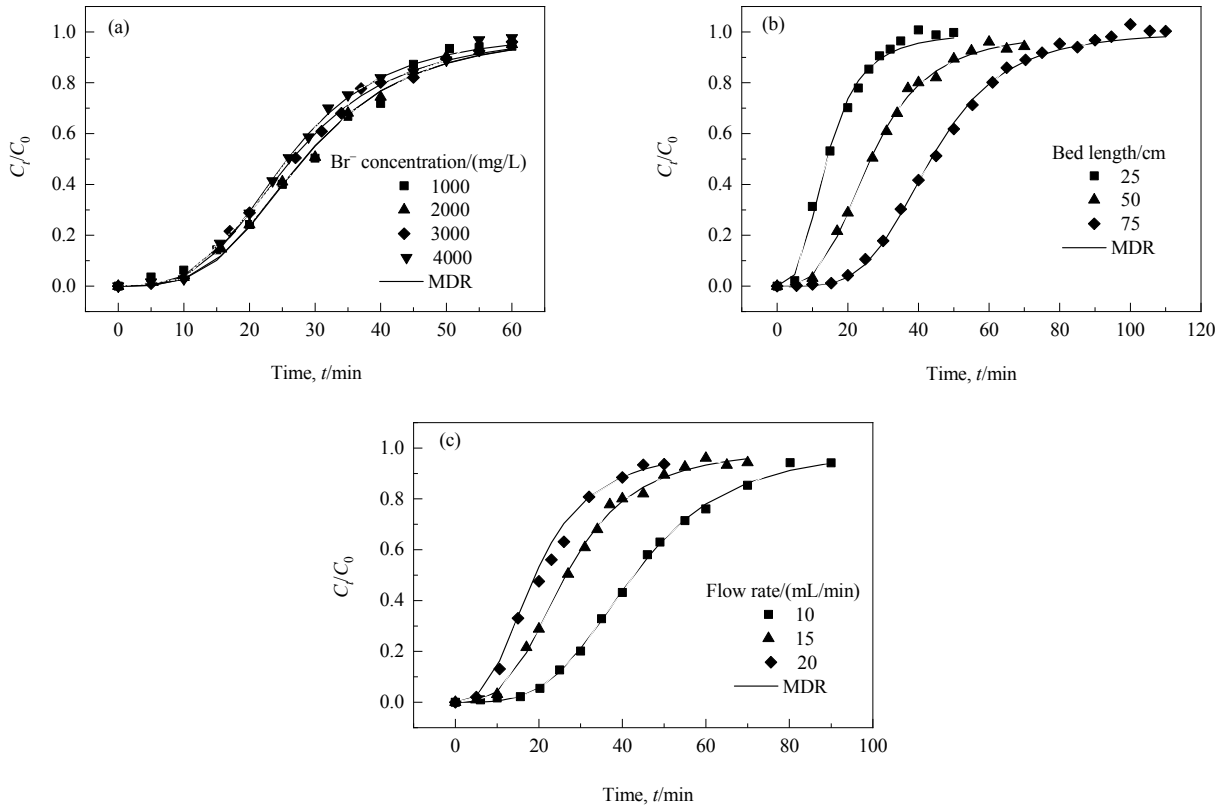

Fig.7 Comparisons of experimental and theoretical breakthrough curves for the adsorption process using the Modified dose response model

Therefore, Wolborska model is not advisable to be applied to describe the adsorption behaviors in fixed-bed column of this study.

4.5.3 Analysis using MDR model

A good fitting between the experimental and theoretical breakthrough curves is also shown in Figure 7. The values obtained using the MDR model are listed in Table 8. Notably, the values of SSE values are quite low and the values of R^2 are very high. The MDR model parameter (a) remained almost the same with the change of initial concentration, but increased with the increase of bed length and decreased with the increase of flow rate. In contrast, the equilibrium adsorbate uptake (q_0) increased with the increase in the initial concentration, bed length, and the decrease in the flow rate.

After comparison of the MDR model with other four models, this model has the lowest values of SSE and the highest values of R^2. Meanwhile, it is clear that the correlation between the experimental and theoretical curves using the MDR model is ideal for all the range of the relative concentration. Hence, it can be concluded that MDR model represents the adsorption behavior of bromide ions onto D301 anion exchange resin much better than the other four models.

Table 8 Parameters of Modified dose response model for bromide adsorption

C_0/(mg/L)	H/cm	Q/(mL/min)	q_0/(mg/mL)	a	R^2	SSE
1000	50	15	3.02	3.44	0.99	0.015
2000	50	15	5.54	3.41	1.00	0.0055
3000	50	15	6.76	3.25	1.00	0.0038
4000	50	15	8.96	3.47	1.00	0.0049
3000	25	15	6.35	2.93	0.99	0.0098
3000	75	15	7.05	4.26	1.00	0.0083
3000	50	10	7.21	3.73	1.00	0.0021
3000	50	20	6.43	2.78	1.00	0.0049

5 CONCLUSION

The adsorption process of bromide ions onto D301 anion exchange resin in a Perspex column was studied. The effects of the initial adsorbate concentration, bed length and flow rate were investigated. It was found that the breakthrough time and the exhaust time increased with increasing bed length and decreasing flow rate, whereas they remained almost the same when changing the initial adsorbate concentration. Besides, decreasing the flow rate and increasing the initial adsorbate concentration improved the adsorption performance. The adsorption capacity would increase proportionally with the increase of initial concentration.

Five models were applied to describe experimental data obtained from the dynamic studies performed on fixed-bed column to simulate the breakthrough curves and to determine the corresponding column kinetic constants in this work. Error analysis showed that MDR model was the most suitable one among the five models, which can be used to describe the whole adsorption process accurately.

REFERENCES

[1] Zhu J H, Ma S F, Liu H Y. Analysis and prospects for present status of production and utilization of bromine [J]. Multipurpose Utilization of Mineral Resources, 2004, (2): 36–41.

[2] Ali N, Shahzad K, Rashid M I. Currently used organophosphate and brominated flame retardants in the environment of China and other developing countries (2000–2016) [J]. Environmental Science & Pollution Research, 2017, 24(23): 18721–18741.

[3] Chai Z H, Li M M. Domestic manufacturing process and expectation of bromine industry [J]. Journal of Salt Science and Chemical Industry, 2018, 47(6): 1–4.

[4] Wang G, Li J G. Salt chemical technology [M]. Beijing: Tsinghua University Press, 2016: 344.

[5] Ma H Z, Li Y S, Cheng H D. Metallogenic model and process of the cretaceous potassium-bearing evaporites involving Changdu, Lanping-Simao and Khorat Basin [J]. Journal of Salt Lake Research, 2019, 27(1): 1–11 (in Chinese).

[6] Hansen B T, Wemmer K, Pawling S. Isotopic evidence for a lake cretaceous age of the potash and rock salt deposit at Bamnet Narong, NE Thailand [C]//The Symposium on Geology of Thailand. Thailand: Department of Mineral Resources, 2002: 26–31.

[7] El-Hamouz A M, Mann R. Chemical reaction engineering analysis of the blowout process for bromine manufacture from seawater [J]. Industrial & Engineering Chemistry Research, 2007, 46(10): 3008–3015.

[8] Li Q X, Liu X F, Xu W H. Research and development status of bromine extracting technique [J]. Guangzhou Chemical Industry,

2014, (21): 24–25 (in Chinese).

[9] Zhang Y. PTFE hollow fiber gas membrane-absorption process for extraction of bromine from brine [D]. Tianjin: Tianjin University, 2015: 39–46 (in Chinese).

[10] Zhang Y, Qin Y J, Liu Q. PTFE hollow fiber supported gas membrane process for extraction of bromine from brine [J]. Chemical Industry and Engineering, 2016, 33(6): 56–62.

[11] Harada M, Okada T. Solvation structure of bromide ion in anion-exchange resins [J]. The Journal of Physical Chemistry B, 2002, 106(1): 34–40.

[12] Wang Y X. The application of strongly basic anion exchange resin in bromine extraction from seawater [D]. Qingdao: Ocean University of China, 2011: 41–63 (in Chinese).

[13] Phetrak A, Lohwacharin J, Sakai H. Simultaneous removal of dissolved organic matter and bromide from drinking water source by anion exchange resins for controlling disinfection by-products [J]. Journal of Environmental Sciences, 2014, 26(6): 1294–1300.

[14] Gurgel A, Vinicius L, Silva M D, et al. Modeling adsorption of copper(II), cobalt(II) and nickel(II) metal ions from aqueous solution onto a new carboxylated sugarcane bagasse. part II: optimization of monocomponent fixed-bed column adsorption [J]. Journal of Colloid and Interface Science, 2018, 516(5): 431–445.

[15] Mondal M K. Removal of Pb(II) ions from aqueous solution using activated tea waste: adsorption on a fixed-bed column [J]. Journal of Environmental Management, 2009, 90(11): 3266–3271.

[16] Nur T, Shim W G, Loganathan P, et al. Nitrate removal using Purolite A520E ion exchange resin: batch and fixed-bed column adsorption modelling [J]. International Journal of Environmental Science and Technology, 2015, 12(4): 1311–1320.

[17] Singh P, Bajpai J, Bajpai A K, et al. Fixed-bed studies on removal of arsenic from simulated aqueous solutions using chitosan nanoparticles [J]. Bioremediation Journal, 2011, 15(3): 148–156.

[18] Yina C Y, Arouab M K, Daud W M A W. Fixed-bed adsorption of metal ions from aqueous solution on polyethyleneimine-impregnated palm shell activated carbon [J]. Chemical Engineering Journal, 2008, 148(1): 8–14.

[19] Ko D C K, Porter J F, McKay G. Optimized correlations for the fixed-bed adsorption of metal ions on bone char [J]. Chemical Engineering Science, 2000, 55(23): 5819–5829.

[20] Kofaa G P, NdiKoungoua S, Kayema G J, et al. Adsorption of arsenic by natural pozzolan in a fixed bed: determination of operating conditions and modeling [J]. Journal of Water Process Engineering, 2015, 6: 166–173.

[21] Malkoc E, Nuhoglu Y. Fixed bed studies for the sorption of chromium (VI) onto tea factory waste [J]. Chemical Engineering Science, 2006, 61(13): 4363–4372.

[22] Noreen S, Bhatti H N, Farrukh Z, et al. Continuous fixed bed removal of Novacron orange P-2R using sugarcane bagasse: prediction of breakthrough curves [J]. Desalination and Water Treatment, 2016, 57(27): 12814–12821.

[23] Yaguba M T, Sena T K, Afrozea S, et al. Fixed bed dynamic column adsorption study of methylene blue (MB) onto pine cone [J]. Desalination and Water Treatment, 2015, 55(4): 1026–1039.

[24] Rao K S, Anand S, Venkateswarlu P. Modeling the kinetics of Cd(II) adsorption on Syzygium Cumini L leaf powder in a fixed bed mini column [J]. Journal of Industrial and Engineering Chemistry, 2011, 17(2): 174–181.

[25] Saadi Z, Saadi R, Fazaeli R. Fixed-bed adsorption dynamics of Pb (II) adsorption from aqueous solution using nanostructured γ-alumina [J]. Journal of Nanostructure in Chemistry, 2013, 3(1): 48–55.

[26] Priya P G, Basha C A, Ramamurthi V. Removal of Ni(II) using cation exchange resins in packed bed column: prediction of breakthrough curves [J]. Clean-Soil, Air, Water, 2011, 39(1): 88–94.

[27] Srivastava V C, Prasad B, Mishra I M, et al. Prediction of breakthrough curves for sorptive removal of phenol by bagasse fly ash packed bed [J]. Industrial & Engineering Chemistry Research, 2008, 47(5): 1603–1613.

[28] Recepoğlua Y K, Kabaya N, Ipeka I Y, et al. Packed bed column dynamic study for boron removal from geothermal brine by a chelating fiber and breakthrough curve analysis by using mathematical models [J]. Desalination, 2018, 437(5): 1–6.

[29] Langmuir I. The constitution and fundamental properties of solids and liquids. part I. solids [J]. Journal of the American Chemical Society, 1916, 38(11): 2221–2295.

[30] Freundlich H. Über die adsorption in lösungen [J]. Zeitschrift fur Physikalische Chemie, 1906, 57(A): 385–470.

[31] Lin Z, Lopes C B, Pereira E, et al. Fixed-bed removal of Hg^{2+} from contaminated water by microporous titanosilicate ETS-4: experimental and theoretical breakthrough curves [J]. Microporous and Mesoporous Materials, 2011, 145(1/2/3): 32–40.

[32] Lin X Q, Li R J, Wen Q S, et al. Experimental and modeling studies on the sorption breakthrough behaviors of butanol from aqueous solution in a fixed-bed of KA-I resin [J]. Biotechnology and Bioprocess Engineering, 2013, 18(2): 223–233.

[33] Malkoc E, Nuhoglu Y, Abali Y. Cr(VI) adsorption by waste acorn of *Quercus ithaburensis* in fixed-beds: prediction of breakthrough curves [J]. Chemical Engineering Journal, 2006, 119(1): 61–68.

[34] He B L, Wang W Q. Adsorption and ion exchange [M]. Shanghai: Shanghai Scientific & Technological Education Publishing House, 1995: 146 (in Chinese).